



ANALYSIS OF THE Mg-Al ALLOY MICROSTRUCTURE OF AZ91

Abstract

The purpose of this work is to demonstrate the crystallization process of Mg-Al alloy with the AZ91 alloy as the example. The work describes various factors, which influence the shaping of the microstructure components in AZ91. The understanding of the factors influencing the microstructure during its development is cognitively crucial, and along with the development of computing it may contribute to forecasting the microstructure in the AZ91 crystallization.

Keywords: AZ91 alloy, microstructure of Mg-Al alloys

1. Introduction

The most wide-spread commercial magnesium alloys are the Mg-Al alloys [1]. The most frequently used alloys of this group are AZ91, AM60 and AM50, albeit to a lesser degree. The AZ91 alloy contains 9% of Al by weight and 1 % of zinc by weight. The zinc increases the alloy's strength in ambient temperature and its flowing power [1].

Due to their mechanical properties at low density, the Mg-Al alloys and composites, enhanced with silicon carbides, are used in the space and automotive industries. The increased interest in the material makes the authors inclined to explore the subject proposed here.

2. The microstructure and phase transition of the Mg-Al alloy

During the crystallization of Mg-Al alloys several components of their structures are created. Identification of the microstructure elements is possible by analyzing the magnesium-aluminium phase equilibrium chart (see fig. 1).

¹ Dr inż. Janusz LELITO,
M.Sc. Paweł ŻAK,
Prof. Józef Szczepan SUCHY,

² Prof. Stanisław RZADKOSZ,

- Department of Mould Materials, Mould Technology and Foundry Engineering of Non-Ferrous Metals in Faculty of Foundry Engineering AGH

³ Dr Halina KRAWIEC,

- Department of Chemistry and Corrosion of Metals, Faculty of Foundry Engineering AGH

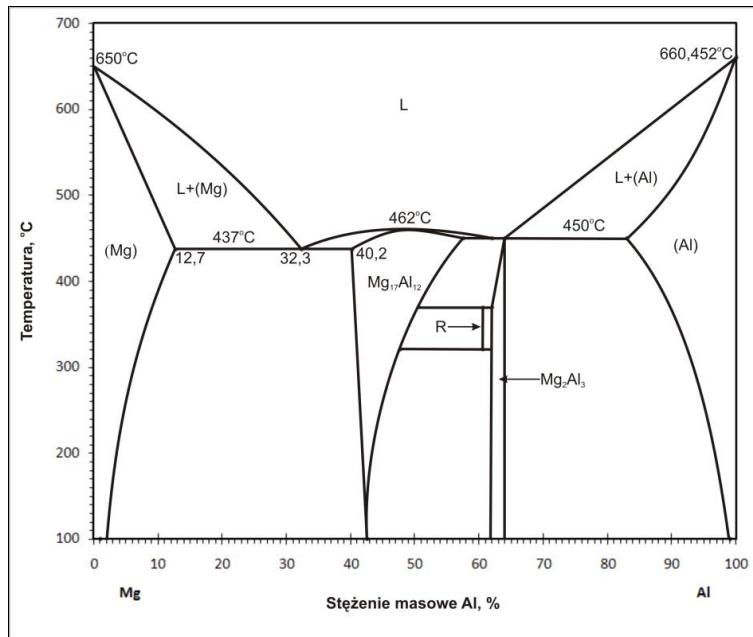


Fig. 1. The Mg-Al phase equilibrium chart [2]

The maximum solubility of aluminium at a eutectic temperature and in solid phase is approximately 13 % of Al by weight. The eutectic composition constitutes around 33 % of Al by weight and falls between the solid α -Mg solution and the intermetallic phase of β -Mg₁₇(Al, Zn)₁₂. The aluminium content of all commercial alloys, which AZ91 can be included into, does not exceed the maximum solubility of aluminium in the solid solution (α -Mg). That is why these alloys crystallize with the magnesium primary phase. The equilibrium phase for all alloys is always the solid α -Mg solution, but during solidification a nonequilibrium (i.e. meta-stable) eutectic is also created and present in the Mg-Al alloy cast microstructure from 2% of Al content by weight. The phenomenon is confirmed by the AZ91 self-cooling curve (see fig. 2). The curve displays a wave at about 600°C, responsible for the nucleation of the α -Mg primary phase, and an arrest at about 430°C, associated with the nonequilibrium crystallization of the eutectic.

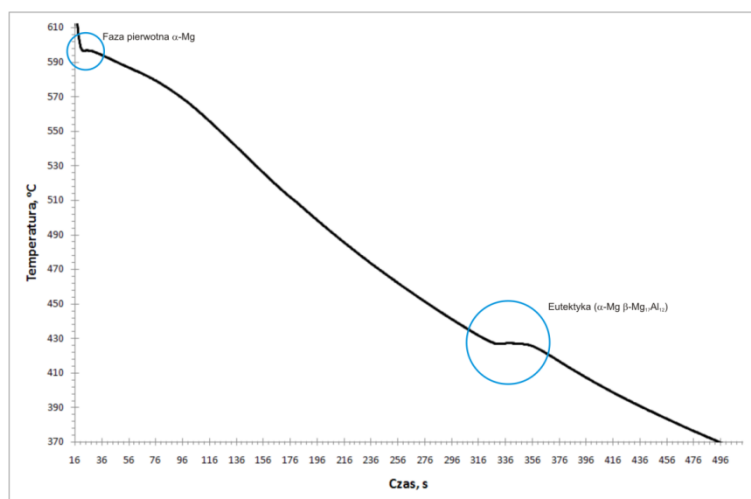


Fig. 2. The AZ91 self-cooling curve for the cast in a high-silica sand & resin mould

The X-ray diffraction examination of the AZ91 alloy (see fig. 3) also confirms the presence of the magnesium primary phase (α -Mg) and the β -Mg₁₇(Al, Zn)₁₂ phase in the microstructure.

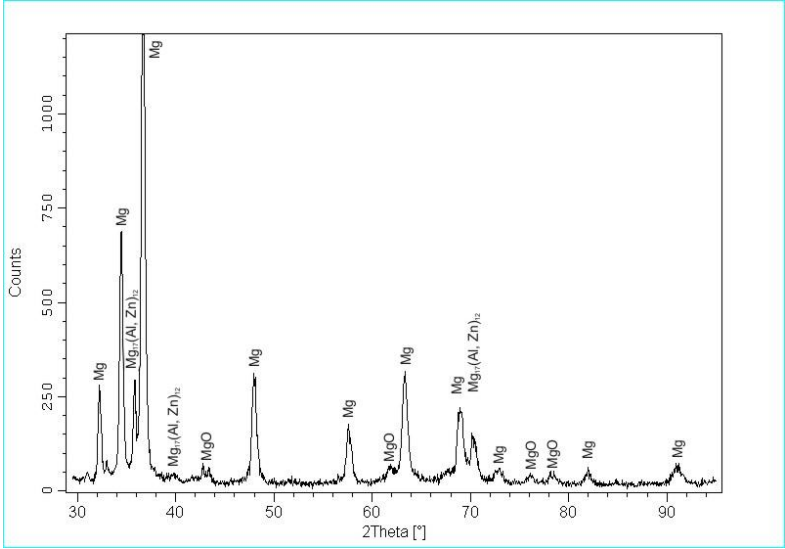


Fig. 3. The XRD pattern of the AZ91 alloy

The crystallization of the AZ91 alloy leads to a structure composed of primary dendrites and the eutectic. Moreover, due to the presence of manganese the AlMn phase is also created during the crystallization process (see fig. 4). The crystallization of this phase is connected with segregation of Al and Mn in the liquid during the increase in the magnesium primary phase. This phenomenon is confirmed by the analysis of chemical composition in area 1 of the precipitate (see fig. 4), where approximately 39.443% of Al by weight and 51.689% of Mn by weight were found. Due to its low lattice disregistry - of about 4% - the AlMn phase can act as the base surface for heterogeneous nucleation of the α -Mg primary phase [3].

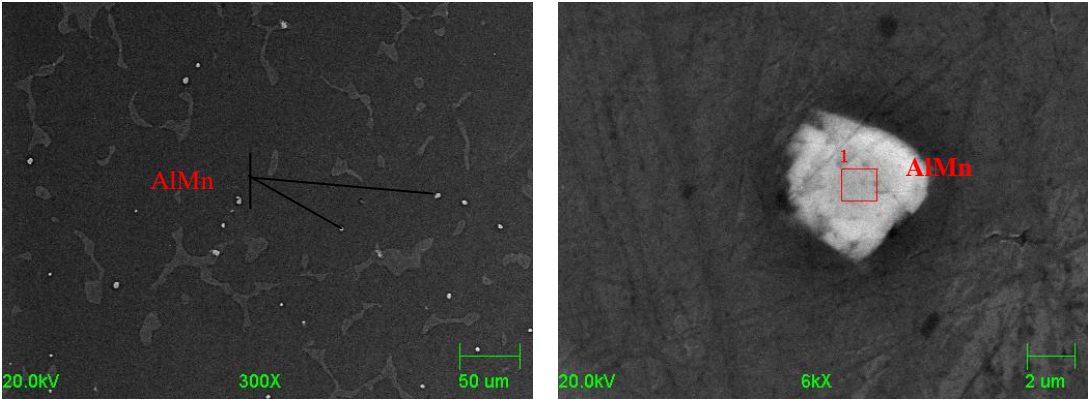


Fig. 4. SEM imaging of the AZ91 alloy with visible AlMn precipitations

The Mg-Al alloys with over 20 % of Al by weight have a regular eutectic, where both phases are non-walled [1]. The volume fraction of the eutectic decreases in direct proportion to the reduction of the Al content, while the eutectic morphology gradually transforms into a divorced eutectic [1]. Heat processing of these alloys may lead to complete dissolution of the β -Mg₁₇(Al, Zn)₁₂ intermetallic phase.

Mg-Al alloys, including AZ91 naturally, exhibit a wide range of solidification temperatures (see fig. 1) and thus are susceptible to casting defects caused by segregation and porosity. The defects assume the shape of stripes parallel to the cast surface (see fig. 5).

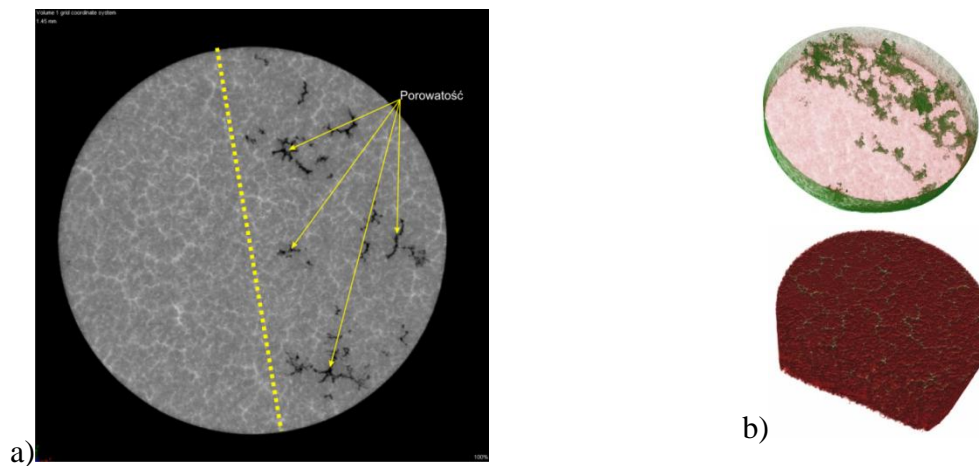


Fig. 5. 2D (a) and 3D (b) computer tomography imaging of the microstructure and porosity of an AZ91 cast

To sum up, we may divide the AZ91 casts solidification into two stages. The first stage begins with the nucleation of the α -Mg primary phase, the grain refinement and its growth. The second stage involves the crystallization of the eutectic, which may have different ranges and morphology.

2.1. The nucleation and growth of the α -Mg primary phase

Solidification of Mg-Al alloys starts with the nucleation of the α -Mg magnesium primary phase at temperatures between 650 - 600°C, beginning from the melting point of pure magnesium to the liquidus temperature overlapping the aluminium content of the most popular commercial Mg-Al with 9% of Al by weight (AZ91). The later solidification stage involves crystallization of the α -Mg + β -Mg₁₇(Al, Zn)₁₂ eutectic, which occurs at 437°C. A typical microstructure of the AZ91 alloy is presented in figure 6, with well-developed dendrites of the α -Mg primary phase characterized by the six-fold symmetry axis.

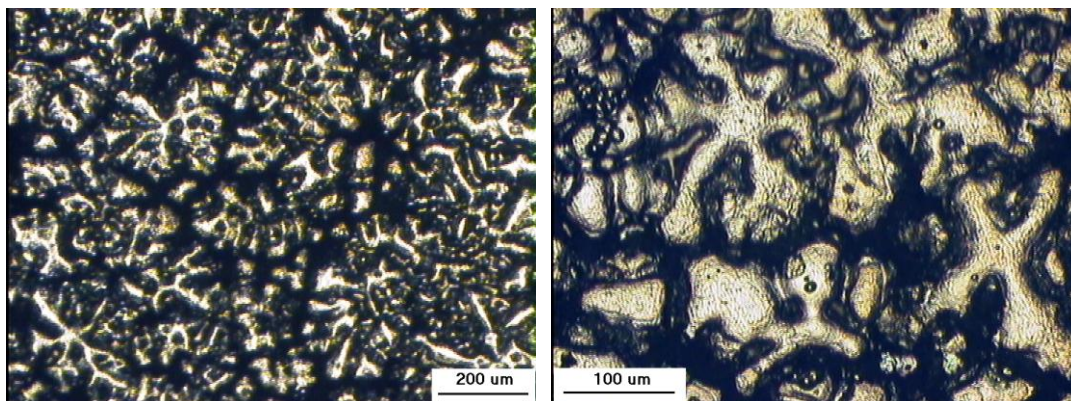


Fig. 6. The AZ91 alloy microstructure with dendritic precipitations of the α -Mg primary phase

The authors of one work [1] reveal the change in the Mg-Al microstructure alloys with the addition of aluminium (Mg-1Al, Mg-3Al, Mg-5Al, Mg-9Al). Even small quantities of aluminium, when added to pure magnesium, lead to changes in the morphology of the primary phase, which transits from cellular to dendritic. The globular equiaxial, rosette-shaped crystallites arise from a solid solution enriched with aluminium between the dendrite arms. Upon increasing the aluminium content to 5 % by weight of the Mg-Al alloy, the dendrites with eutectic areas between the arms begin to expand into a fully-developed dendritic structure (fig. 6), at the aluminium content of about 9% of Al by weight.

Grain refining is one of the methods aimed at enhancing the mechanical properties of casts. The grain size is usually established in the early stages of the solidification process by the nucleation of the dendrite grains. The first method which enables grain refining involves quick cooling of molten metal to the desired temperature following a short holding at an increased temperature (usually between 150 and 260°C) above the equilibrium liquidus temperature [1]. Despite the success at grain refining with this method, alternative technologies were pursued due to several practical problems which mostly involve higher operating temperature. Another method of grain refining relates to the introduction of iron(III) chloride (with the Elfinal process) into magnesium alloys which contain aluminium and manganese. The resulting grain size is somewhat similar to the sizes obtained by overheating the alloy [1]. However, due to the decreased resistance to corrosion, caused by iron, the Elfinal process did not attract much attention from the industry.

Yet another method used to refine the grain is based on introducing carbon into the molten alloy (i.e. seeding with carbon). This method has practical benefits at lower operating temperatures. Various carbon additives, i.e. organic materials (C_2Cl_6 , CCl_4) [1], granulated graphite [1] or silicon carbide particles (SiC) [1, 4 – 6] lead to effective grain refining of magnesium-aluminium alloys.

In order to understand the grain refining mechanism, the interaction of basic factors, i.e. identification of active nuclei and/or alloy additions with tendencies towards strong segregation must be understood first.

Recent works [1, 8] on grain refining of aluminium alloys demonstrate that the process can be affected with two mechanisms. The first consists in creation of crystals in the thermally overcooled area near the casting mould walls in the early stages of casting. Then the convection currents carry the crystals deeper into the molten metal. The second mechanism results from concentrative overcooling, generated by the increase of grain on a plate suspended in molten metal [1, 8]. Both techniques increase the number of crystallization nuclei. In the first case the process is affected mainly by the alloy additions present in the molten alloy, while in the other the number and the nucleic potential of the plate (ΔT_n). The authors placed a figure in their work [1] to exhibit the influence of both factors on the grain refining. It is implicated that in the case of plates within the alloy just a small quantity of alloy additives contributes to a rapid decrease in the grain size, while any further increase in the alloy additives does not influence grain refining much more.

As a result of solidification, when the plate power is very high, the effect of an alloy additive may be described by the growth restriction factor (GRF) [7]. The GRF is defined with the following formula: $Q = \sum_i m_i C_{0,i} (k_i - 1)$, where m is the liquidus line gradient coefficient, C_0 is the initial concentration of alloy components and k_i is the equilibrium division coefficient of i , i.e. the alloy component [7]. A high value of the growth restriction factor induces rapid concentrative overcooling by the developing crystal, so the liquid adhering around the plate reaches an overcooling state more quickly and enough for a solid nucleus to be formed on the plate, in comparison to alloys with low GRF. This means that with a high plate power a low overcooling value is required for the development of crystallization nuclei. Combined with the chemical composition of the liquid alloy and a high

growth restriction factor, the high power of the plates may lead to the development of small grains. Several alloy additions, i.e. aluminium, calcium, silicon and zircon, have strong segregation properties and thus lead to significant grain refining in pure magnesium [1]. In the case of magnesium-aluminium alloys however, the admixture of zircon is not effective at grain refining due to its unfavourable interaction with aluminium.

The conclusion drawn from the aforementioned mechanism of the primary phase nucleation is that if all components of an alloy are transformed into corresponding growth restriction factors, and the number and power of plates are equal, the grain size dependent on the GRF should be the same for all alloys. This thesis is true – but only for binary magnesium alloys with Si, Ca and Zr. In the case of binary alloys of magnesium and aluminium this is invalid. The plates in the Mg-Al alloys have very small potential and Mn increases the alloy grain size [1]. Moreover, the grain size changes significantly depending on the purity of ingots used to prepare the alloy [1].

The addition of SiC, AlN and Al₄C₃ to magnesium alloys cause grain refining, since all these molecules have small lattice disregistry in relation to magnesium and therefore constitute a good base for heterogeneous nucleation of magnesium.

2.2. Nucleation and the eutectic growth

As mentioned earlier, the self-cooling rate of the alloy is enough to create the eutectic during the solidification of magnesium alloys containing over 2% of Al by weight [1]. That is why the AZ91 casts contain a significant volume fraction of eutectic. There are two reasons which make understanding of the eutectic solidification process important. First, the solidification process controls the volume, shape and displacement of the very fragile β -Mg₁₇(Al, Zn)₁₂ phase which appears in the final microstructure and affects the flow and creep strength of these alloys [1]. Second, the growth of the eutectic at the final stage of the solidification process influences the capability of feeding the interdendritic areas, where high partial pressures are required for the fluid to flow through the dendrite lattice. The differences in the way the eutectic grows have a significant effect on the ease of the fluid to flow through the dendritic lattice and therefore affect the creation of pores in the casts.

According to the Mg-Al phase equilibrium chart (see fig. 1) the β -Mg₁₇(Al, Zn)₁₂ eutectic phase appears in the microstructure when the aluminium content of the alloy is increased to approximately 13 % by weight.

The eutectic phase can also be present in alloys with 2% of aluminium by weight - the phenomenon is attributed to a nonequilibrium crystallization process. The eutectic and the β -Mg₁₇(Al, Zn)₁₂ phase are present in the metallographic imaging of the AZ91 alloy (see fig. 7). Both components of the microstructure are crystallized at the boundaries of the α -Mg primary phase dendrites. The darker areas by the dendrite boundaries indicate aluminium content larger than in the lighter areas of the magnesium primary phase.

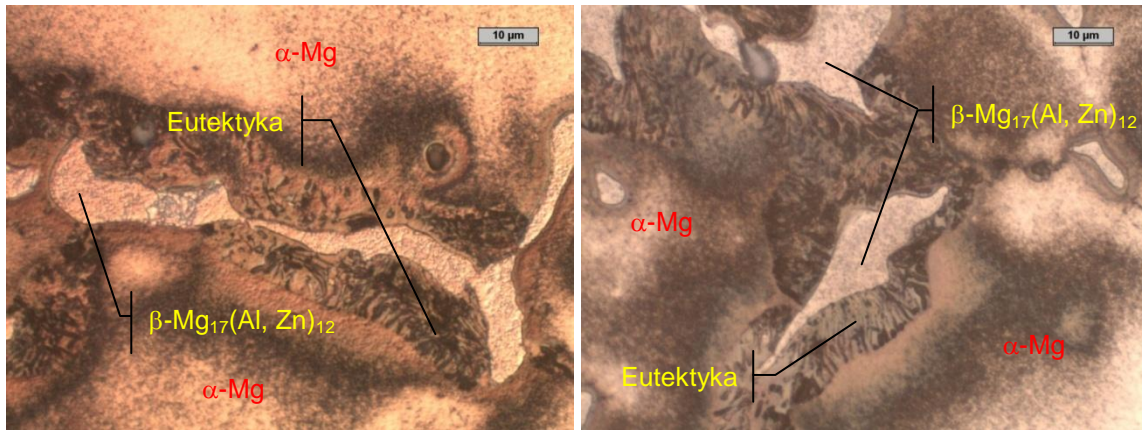


Fig. 7. The AZ91 alloy microstructure with visible eutectic and intermetallic solution

In order to identify the components created within the microstructure of AZ91 examinations with a Scanning Electron Microscope have been carried out to analyze the chemical composition of three different areas which represent three different structural components (see fig. 8).

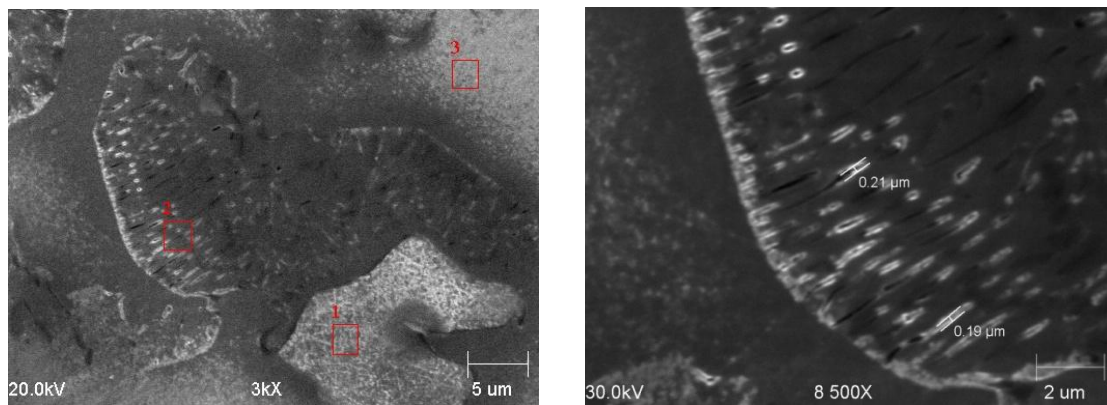


Fig. 8. SEM imaging of the AZ91 alloy microstructure with visible structural components

The results of the analyses are demonstrated in Table 1. Area 1 contains the lowest magnesium content (approx. 59% by weight) with the largest zinc fraction (approx. 4.5% by weight) and aluminium (approx. 36% by weight). This chemical composition suggests that area 1 belongs to the $\beta\text{-Mg}_{17}(\text{Al}, \text{Zn})_{12}$ phases. The highest magnesium content (approx. 96% by weight) with the lowest aluminium concentration (approx. 3 % of weight) and practically trace zinc content is in area 3. Such concentration of elements may indicate the $\alpha\text{-Mg}$ primary phase. Due to the percentage fraction of particular elements (see Table 1), area 2 is where the eutectic ($\alpha\text{-Mg} + \beta\text{-Mg}_{17}(\text{Al}, \text{Zn})_{12}$) is present. The eutectic itself has a dispersion of approximately 0.2 μm (see fig. 8).

Table 1

Chemical composition analysis of three areas

Area no.	The percentage content of the AZ91 alloy components		
	Mg [% by weight]	Al [% by weight]	Zn [% by weight]
1	59.434	36.015	4.551
2	89.261	8.826	1.913
3	96.338	3.245	0.418

Surface and linear analysis of the element distribution have also been conducted. Analysis included the $\beta\text{-Mg}_{17}(\text{Al}, \text{Zn})_{12}$ phase surrounded by the $\alpha\text{-Mg}$ primary phase. The results are shown in figs. 9 and 10. The linear analysis reveals a decrease in the magnesium content, from approx. 95% by weight in the $\alpha\text{-Mg}$ phase to approx. 60% by weight in the $\beta\text{-Mg}_{17}(\text{Al}, \text{Zn})_{12}$ (see fig. 9). As for aluminium and zinc, the concentration variations proceed inversely: the aluminium content increases from approx. 5% by weight in the $\alpha\text{-Mg}$ phase to about 37% by weight in the $\beta\text{-Mg}_{17}(\text{Al}, \text{Zn})_{12}$ phase.

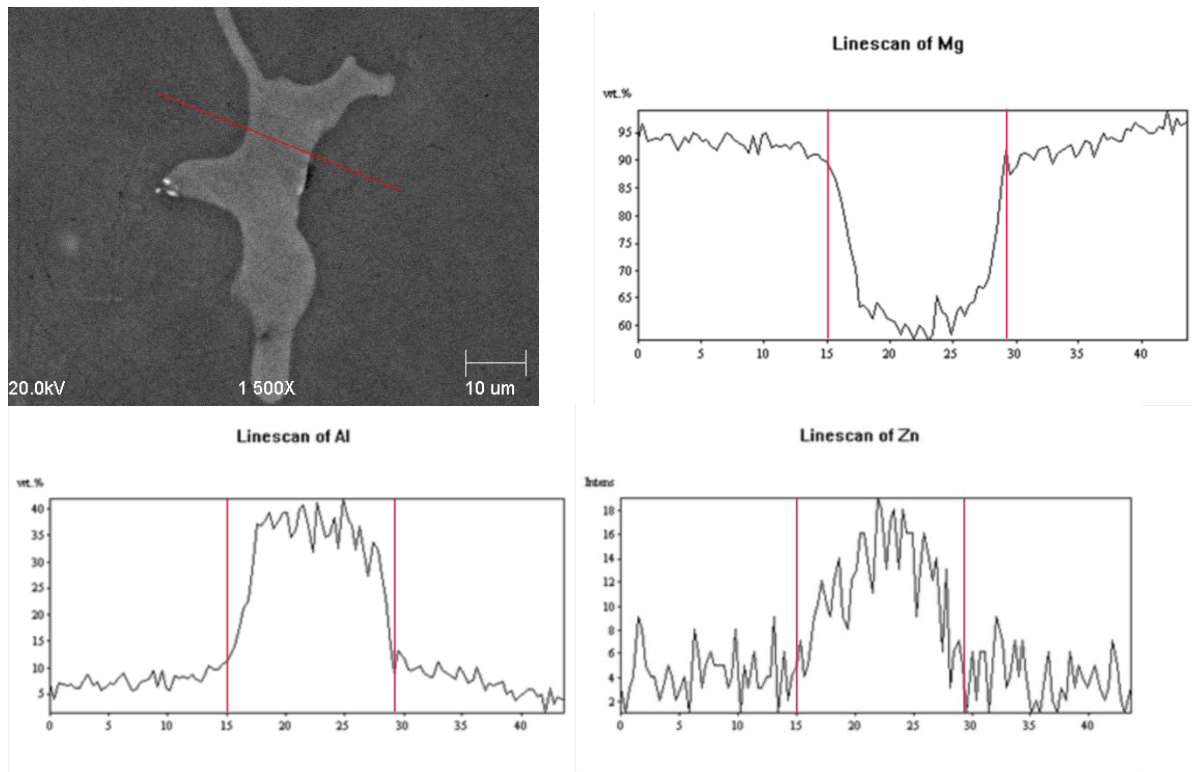


Fig. 9. Linear analysis of Mg, Al and Zn distribution in the $\alpha\text{-Mg} - \beta\text{-Mg}_{17}(\text{Al}, \text{Zn})_{12} - \alpha\text{-Mg}$ configuration

Following the surface distribution of Mg, Al and Zn (fig. 10) it is revealed that both aluminium and zinc tend to concentrate in the precipitate, while magnesium is concentrated in the $\alpha\text{-Mg}$ primary phase.

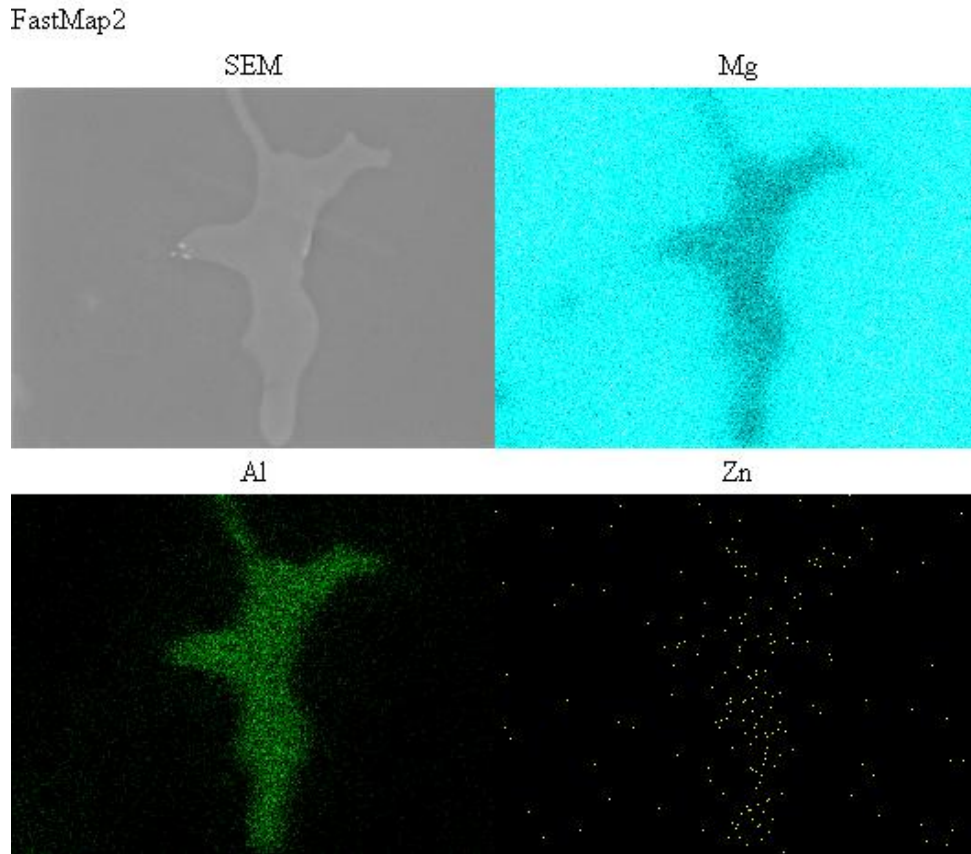


Fig. 10. Surface analysis of Mg, Al and Zn distribution in the α -Mg – β -Mg₁₇(Al, Zn)₁₂ – α -Mg configuration

The eutectic exhibits a wide range of different morphologies within the hypoeutectic Mg-Al alloys, depending on the chemical composition and the self-cooling rate [1]. The alloys with the aluminium content reaching the eutectic level (i.e. 33% of Al by weight) tend to develop the eutectic of regular lamellar or fibrous morphology [1], while the alloys with less than 10% of Al by weight display partially or completely divorced eutectic. A completely divorced morphology occurs when the two phases within the eutectic grow separately without direct exchange of substances dissolved between the phases. In such a case every interdendritic area is composed of singular precipitates of the β -Mg₁₇(Al, Zn)₁₂ phase, surrounded by the eutectic phase of α -Mg which grew from the primary dendrites. A partially divorced eutectic is characterized by precipitates forming islets of the α -Mg phase within the β -Mg₁₇(Al, Zn)₁₂ phase, while most of the α -Mg phase remains outside the precipitates of β -Mg₁₇(Al, Zn)₁₂, which means that the volume fraction of the α -Mg phase within the β -Mg₁₇(Al, Zn)₁₂ precipitates is much smaller than would have been indicated proportionally by the phase equilibrium chart.

The effect of the aluminium and zinc contents and the self-cooling rate on the eutectic morphology at the casting stage is shown in the diagram below (see fig. 11). The eutectic tends to become less divorced as the aluminium content increases, and becomes more divorced as the zinc content and self-cooling rate increase.

The major mechanisms behind the influence of the chemical composition and self-cooling on the eutectic morphology are related to the location of the compressed zone and overcooling during the solidification [1].

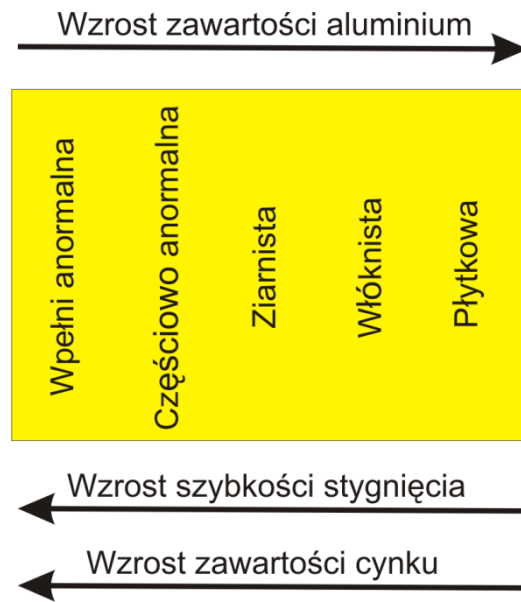


Fig. 11. The effect of the aluminium and zinc content, as well as the self-cooling rate on the eutectic morphology of hypoeutectic Mg-Al alloys [1]

The morphology and the eutectic crystallization mechanism is important to the feeding capacity during the final, critical stage of solidification. Independent nucleation and growth of the $\beta\text{-Mg}_{17}(\text{Al}, \text{Zn})_{12}$ within the interdendritic areas will probably dramatically increase the proportion of the surface to the feeding channels and obstruct the feeding of these areas. On the other hand, however, the nucleation of the $\beta\text{-Mg}_{17}(\text{Al}, \text{Zn})_{12}$ phase on $\alpha\text{-Mg}$ and their following growth towards the centre of the interdendritic channels should allow a feeding path which would feed the solidifying areas as the last and thus allowing a sound, non-porous casting.

The feeding during the eutectic's solidification will include the solidification range of the eutectic and the smoothness of the solid/liquid separation surface during the eutectic growth (i.e. if one of the phases is the leading one, growing before the other during the compressed growth), or the feeding is like an isothermal interface of the eutectic growth. A smooth, isothermal interface facilitates the feeding, while an interface in which one of the phases is significantly more advanced than the other would require feeding along ever narrower and convoluted pathways to avoid porosity. Zinc present in the AZ91 alloy is an element strongly segregated into the $\beta\text{-Mg}_{17}(\text{Al}, \text{Zn})_{12}$ phase during the growth of the eutectic (fig. 9, 10), thus greatly advancing the $\alpha\text{-Mg}$ phase, and contributes to solidification of the eutectic with a smaller isothermal interface [1]. Based on the abovementioned it is concluded that the addition of zinc contributes to the porosity of casts.

2.3. Precipitation reactions

The end of the eutectic's solidification does not necessitate the end of phase changes in casted Mg-Al alloys [1]. When the alloy self-cooling rate is slow enough (i.e. typical for sand mould casting) the precipitates may appear in supersaturated areas of the $\alpha\text{-Mg}$ phase. The precipitate can be linear (see fig. 12 [A]) or discrete (see fig. 12 [B]).

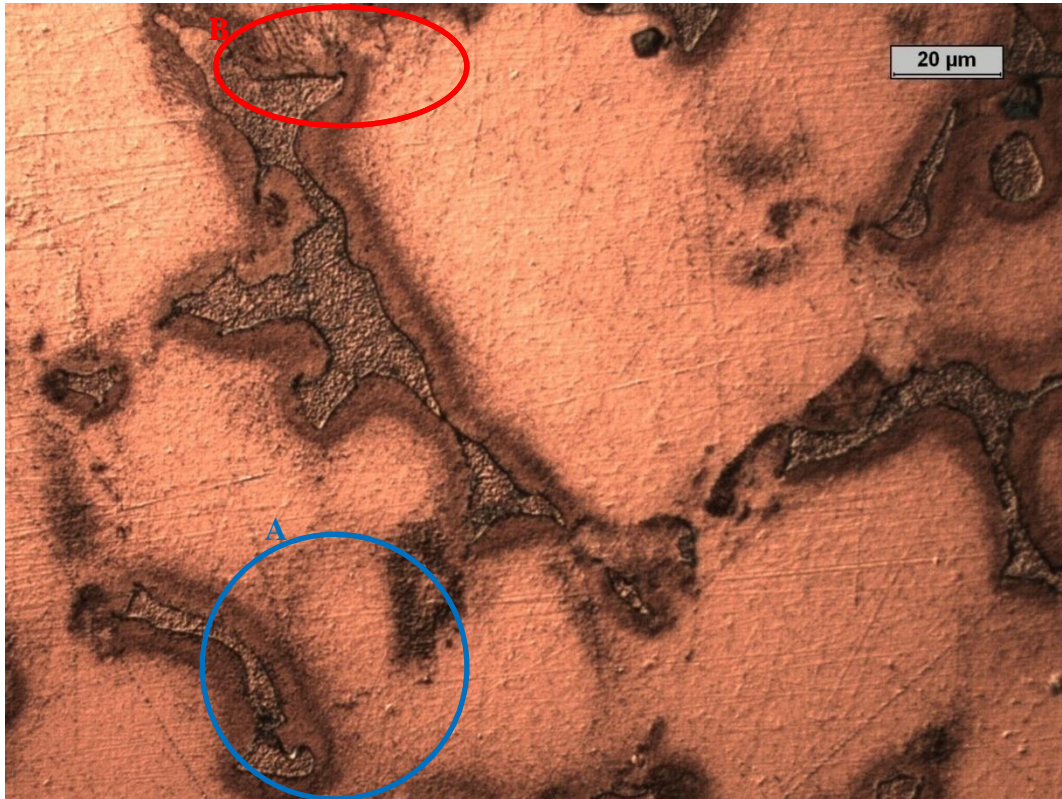


Fig. 12. Metallographic imaging of the AZ91 alloy microstructure with linear (A) and discrete precipitates (B)

Discrete precipitates induce the growth of lamellar precipitates of $Mg_{17}Al_{12}$ within the α -Mg crystallites, similar to pearlite growing inside austenite crystallites upon cooling steel. Aluminium separates the lamellar $Mg_{17}Al_{12}$ precipitates during their growth, leaving the aluminium-depleted α -Mg phase between the lamellas. The discrete precipitates grow from the eutectic $Mg_{17}(Al, Zn)_{12}$ phase towards the insides of the α -Mg crystallites. The discrete precipitates occur mainly in the areas of the α -Mg primary phase, near the $Mg_{17}(Al, Zn)_{12}$ phase, all due to higher aluminium content within the area (i.e. approx. 10 to 13% of Al by weight) than the dendrite centres of α -Mg, where the aluminium levels may be as low as 2% of Al by weight [1].

3. Porosity

Solidification of Mg-Al alloys is important to the microporosity development process. The causes of microporosity in Mg-Al have been the subject of numerous discussions and much scientific research [1]. The major topic of these discussions was the question whether microporosity is induced by a contraction during the solidification of alloys, or is rather related to the content of dissolved hydrogen.

The initial findings would produce a conclusion that microporosity is not caused by dissolved hydrogen. The differences in hydrogen solubility between the solid and liquid states of Mg-Al alloys are relatively small when compared to aluminium alloys and that is why it was assumed that the contraction was the cause. The theory was soon refuted, and the experimental measurements of hydrogen content in liquid casts prior to solidification would suggest that it is the dissolved hydrogen that contributes to microporosity [1].

However it is impossible that the microporosity of Mg-Al alloys is connected to just one of the aforementioned mechanisms. The solidification contraction and the release of

dissolved hydrogen occur simultaneously and cause the microporosity [1]. Magnesium alloys solidify relatively more slowly than aluminium alloys due to their low thermal conduction. That is why gradual feeding of interdendritic areas is difficult and yet because of the wide range of solidification temperatures it remains a crucial stage of solidification of magnesium alloys [1, 4 – 6].

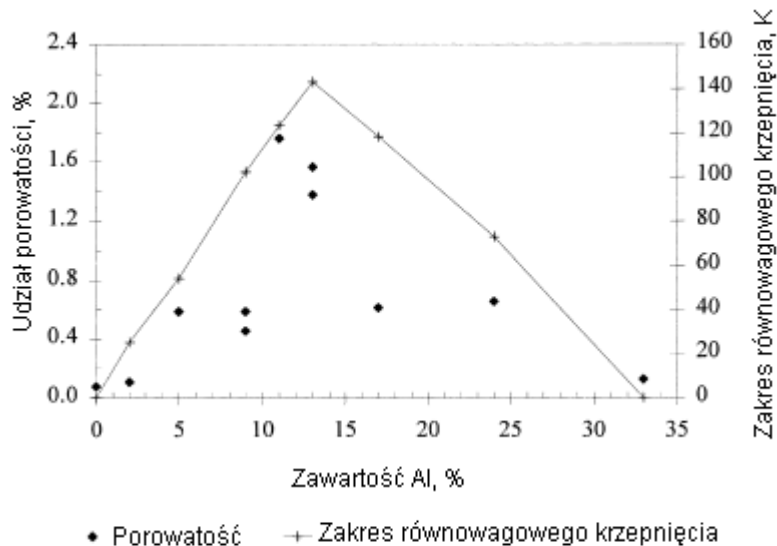


Fig. 13. Effect of aluminium content and the equilibrium solidification range on the porosity fraction [1]

Fig. 13 demonstrates the strong effect of aluminium content on the porosity volume fraction in hypoeutectic Mg-Al alloys. The highest porosity is present in alloys containing approximately 11% of Al by weight, slightly below the maximum equilibrium solidification. Low porosity of pure magnesium and the eutectic alloy (i.e. 33% of Al by weight) is associated with isothermal or near-isothermal solidification of these alloys. Other Mg-Al alloys with their eutectic volume fraction increasing in direct proportion to the aluminium content, starting from 13% of Al by weight, exhibit a decrease in porosity. Maximum porosity is noted at the level of 11% of Al by weight and associated with the worst combination, i.e. the interdendritic areas feeding, the size of the feeding zone and the eutectic volume fraction. When these alloys crystallize there is an insufficient quantity of the fluid to feed the area of contracting eutectic; this causes the porosity to initially increase with the increase of the eutectic volume fraction. As mentioned in the section covering the eutectic growth, the phenomenon is associated with significant changes in the eutectic morphology and the increase of aluminium content. A change in the eutectic morphology and the flow of liquid in the interdendritic areas may result in the growth of porosity.

Conclusion

The solidification process of the AZ91 alloy begins with the nucleation of the α -Mg primary phase dendrites. The α -Mg crystallite size is defined by several factors: self-cooling rate, chemical composition and the type of particles present in the liquid, which may serve as bases for heterogeneous nucleation.

It must be noted that during the crystallization of the primary phase dendrites the AlMn phase also crystallizes, which may serve as a base for heterogeneous nucleation of the α -Mg phase. The effect of the chemical composition on the crystallite size may be determined by the growth restriction coefficient.

The next phase of the AZ91 solidification is the crystallization of the eutectic, which itself is comprised of a mixture of the β -Mg₁₇(Al, Zn)₁₂ phase and the aluminium-rich α -Mg phase. The morphology of the eutectic and the liquid flow in the interdendritic areas may result in the growth of porosity.

Acknowledgements

This work was supported by the Polish Ministry of Science and Higher Education under the grant no N507 446634.

References

- [1] – A. K. Dahle, Y. C. Lee, M. D. Nave, P. L. Schaffer, D. H. StJohn: Development of the as-cast microstructure in magnesium-aluminium alloys. *Journal of Light Metals*, vol. 1, 2001, pp. 61-72.
- [2] – ASM Handbook Committee, *Alloy Phase Diagrams* ASM International, Ohio, USA, 1992.
- [3] – Peng Cao, Ma Qian, David H. StJohn: Effect of manganese on grain refinement of Mg–Al based alloys. *Scripta Materialia*, vol. 54, 2006, pp. 1853–1858.
- [4] – L. Lu, A.K. Dahle, D.H. StJohn: Grain refinement efficiency and mechanism of aluminium carbide in Mg – Al alloys. *Scripta Materialia*, vol. 53, 2005, pp. 517–522.
- [5] – J. Lelito, P. Żak: Simulation of AZ91/SiC composite solidification. *Przegląd Odlewnictwa*, Krakow 2007, nr 3, s. 124-133.
- [6] – L. Lu, A.K. Dahle, D.H. StJohn: Heterogeneous nucleation of Mg–Al alloys. *Scripta Materialia*, vol. 54, 2006, pp. 2197-2201.
- [7] – T.E. Quested, A.T. Dinsdale, A.L. Greer: Thermodynamic modelling of growth-restriction effects in aluminium alloys. *Acta Materialia* vol. 53, 2005, pp. 1323–1334.
- [8] – M. Easton, D. StJohn: Grain Refinement of Aluminium Alloys: Part II. Confirmation of, and a Mechanism for, the Solute Paradigm. *METALLURGICAL AND MATERIALS TRANSACTIONS A* vol. 30A, June 1999, pp. 1625–1633.